Published in final edited form as:
J Magn Reson. 2013 March ; 228: 59–65. doi:10.1016/j.jmr.2012.12.013.

Probing alanine transaminase catalysis with hyperpolarized $^{13}CD_3$-pyruvate

A.W. Barb, **S.K. Hekmatyar**, **J.N. Glushka**, and **J.H. Prestegard***
Complex Carbohydrate Research Center, University of Georgia, 315 Riverbend Road, Athens, GA 30602, United States

Abstract

Hyperpolarized metabolites offer a tremendous sensitivity advantage (>10^4 fold) when measuring flux and enzyme activity in living tissues by magnetic resonance methods. These sensitivity gains can also be applied to mechanistic studies that impose time and metabolite concentration limitations. Here we explore the use of hyperpolarization by dissolution dynamic nuclear polarization (DNP) in mechanistic studies of alanine transaminase (ALT), a well-established biomarker of liver disease and cancer that converts pyruvate to alanine using glutamate as a nitrogen donor. A specific deuterated, ^{13}C-enriched analog of pyruvic acid, $^{13}C3D_3$-pyruvic acid, is demonstrated to have advantages in terms of detection by both direct ^{13}C observation and indirect observation through methyl protons introduced by ALT-catalyzed H–D exchange. Exchange on injecting hyperpolarized $^{13}C3D_3$-pyruvate into ALT dissolved in buffered ^1H_2O, combined with an experimental approach to measure proton incorporation, provided information on mechanistic details of transaminase action on a 1.5 s timescale. ALT introduced, on average, 0.8 new protons into the methyl group of the alanine produced, indicating the presence of an off-pathway enamine intermediate. The opportunities for exploiting mechanism-dependent molecular signatures as well as indirect detection of hyperpolarized ^{13}C3-pyruvate and products in imaging applications are discussed.

Keywords

Nuclear magnetic resonance spectroscopy; Magnetic resonance imaging; Dissolution dynamic nuclear polarization; Metabolic biomarkers

1. Introduction

The introduction of hyperpolarization equipment and methods has extended the ability of solution magnetic resonance methods to characterize low abundance products or transitory processes on previously unimaginably short timescales. It is even possible to observe metabolic conversions of diagnostic value in tissues and living animals. Enhancements exceeding 10^4-fold for directly detected ^{13}C or ^{15}N signals after hyperpolarization by dissolution dynamic nuclear polarization (DNP) [1] have made imaging of cancerous tissues and the monitoring of metabolic flux in living animals possible [2–5]. However, the ability of specific enzymes to imprint mechanism-dependent signatures on metabolic products is yet to be fully exploited. Here we examine some of these signatures in the alanine transaminase catalyzed conversion of pyruvate to alanine.

*Corresponding author. Fax: +1 706 542 4412. jpresteg@ccrc.uga.edu (J.H. Prestegard).

Hyperpolarized pyruvate has emerged as the dominant reagent for imaging tumor morphology and chemistry with magnetic resonance imaging techniques. As such, there is considerable precedent for polarizing and observing pyruvate and its products. Most applications exploit analogs enriched with ^{13}C at the C1 carboxylate or C2 carbonyl sites. These choices arise from the need to prolong storage times of polarization; non-protonated carbons typically have spin relaxation times an order of magnitude longer than protonated carbons. However, as observation at higher field is implemented (something that is particularly useful for mechanistic studies) spin relaxation times at these sites actually decrease due to a magnetic field-dependent chemical shift anisotropy relaxation mechanism. Also, not all substrates have such convenient non-protonated sites. This has spawned an interest in deuterated substrates [6–12]. A typical deuterated site displays spin relaxation times on the order of four fold longer than those for the corresponding protonated substrates, making storage of polarization on deuterated sites competitive with storage on non-protonated sites, particularly at higher magnetic fields [8,10]. The presence of deuterons on the C3 methyl group of pyruvate is something that we will exploit for both prolonged storage and the ability to probe the catalytic mechanism through deuteron (D) for proton (H) exchange. Proton exchange also provides the opportunity to test indirect detection through protons as a means of further enhancing sensitivity.

Pyruvate metabolism is altered in many diseased tissues. Endogenous enzymes convert supplemented pyruvate to lactate (lactate dehydrogenase), acetyl-CoA (pyruvate dehydrogenase), oxaloacetate (pyruvate carboxylase), or L-alanine (alanine transaminase, ALT, E.C. 2.6.1.2). Elevated lactate levels positively correlate with tissue hypoxia, a marker of poorly perfused tumors [13]. Alanine levels likewise rise in tumor tissues as acetyl-CoA production decreases. In addition, ALT activity in the serum is a biomarker for liver damage [14], and could be probed concomitantly with alanine and lactate levels in tumors using hyperpolarized pyruvate. As a preface to potential applications monitoring ALT activity we explore here mechanistic signatures of the enzyme using hyperpolarized $^{13}C3D_3$ pyruvate as well as a more conventional $^{13}C2$ pyruvate as substrates *in vitro*. These signatures may ultimately help differentiate activities of different enzymes when they share a substrate or generate similar products.

The catalytic mechanism of ALT is illustrated in Fig. 1 [15–17]. According to this accepted model of the catalytic mechanism, ALT transfers the amine from glutamate to the pyruvate ketone (C2) carbon forming L-alanine and α-ketoglutarate using pyridoxal phosphate as a coenzyme. In this process the pyruvate C2 site accepts a proton and becomes the alanine Cα. Proton introduction at this and other sites opens opportunities to enhance experimental sensitivity. Assuming equal instrumental efficiency, a 16-fold increase in sensitivity over direct detection of hyperpolarized ^{13}C is expected when using an indirect-detection strategy [10]. Our proposed indirect detection approach stores magnetization on ^{13}C (C2 in this case), transfers polarization to a bonded proton following chemical conversion, and detects the proton signal. Our previous experiments using hyperpolarized $^{15}N(D_2)$ in the sidechain of glutamine as a storage site and indirect detection of $^{15}N(DH)$ demonstrated this method to be 20-fold more sensitive than direct detection of hyperpolarized ^{15}N, compared to the 100-fold maximum expected for that case [10]. Detection of the Cα proton may, however, be more challenging because of more efficient ^{13}C spin relaxation at this site.

In addition to proton incorporation at the pyruvate C2, there is an opportunity to catalyze proton (H)/deuteron (D) exchange at the C3 methyl group and indirectly detect through a protonated alanine product [16,18]. Exchange does not appear obligatory in the production of alanine but may result from a side reaction involving the postulated Schiff base intermediate interconverting with an enamine isoform [17] (denoted in Fig. 1 with a *circled* “A”). The extent to which pathway A (enamine formation, Fig. 1 highlighted in gray) is

sampled compared to pathway B will be reflected in the percentage of proton incorporation in the alanine product. This ratio is very dependent on the nature of the active site and is likely to be very enzyme specific. Here we demonstrate that H/D exchange at the methyl group does occur to a significant extent and that indirect detection of hyperpolarized ^{13}C-labeled pyruvate following ALT-catalyzed H/D exchange is possible.

2. Materials and methods

All materials, unless otherwise noted, were purchased from Sigma– Aldrich (St. Louis, MO). Isotope-enriched chemicals (sodium pyruvate and deuterium oxide) were purchased from Cambridge Isotopes (Cambridge, MA).

2.1. Preparing $^{13}C3D_3$-pyruvate

Sodium pyruvate ($^{13}C3H_3$; 110 mg) was incubated in 20 mL of 25 mM ammonium carbonate, ~95% D_2O, pH 10, for 2 d at 37 °C. The pH was adjusted with ammonium hydroxide. The progress of the reaction was monitored by observing proton and deuteron NMR signals. The solution containing sodium $^{13}C3D_3$-pyruvate was then lyophilized to remove solvent and volatile buffer components.

2.2. Hyperpolarization

For each hyperpolarization experiment, a solution of 800 μg sodium ^{13}C-pyruvate was dissolved with gentle heating to a final concentration of 40 mg/mL in 50/50 (v/v) D_2O/glycerol containing 15 mM OXO63 trityl radical (GE-Healthcare, UK). This mixture was added to a polyether ether ketone (PEEK) plastic cup and lowered into an Oxford Hypersense 3.35T DNP polarizer (Oxfordshire, UK). The sample was cooled to 1.37–1.40 K then irradiated for 1–2 h at 94.007 GHz and 50 mW. The hyperpolarized material was then quickly melted and dissolved in 3.5 mL of pre-heated and pressurized 50 mM sodium phosphate and 10 mM glutamate, pH 8.0 in 100% H_2O. The dissolved material was flushed into a waiting 8 mm NMR tube preloaded with 500 μL of the previous buffer and 10 Units (~70 μg; except where otherwise noted) of porcine heart ALT. This NMR tube was prepositioned inside a Varian 11.7 T INOVA spectrometer (Santa Clara, CA) equipped with an XH probe operating at 31 °C. Sample transfer times were approximately 3 s.

2.3. Detecting nascent alanine

Hyperpolarized $^{13}C3D_3$-pyruvate was transferred to a waiting 8 mm NMR tube loaded with 100 Units ALT and glutamate as described above, and this was followed by a 5 s settling period. Hyperpolarization in the alanine formed to this point was then destroyed by selective, on-resonance, rf irradiation at 29 dB for 500 ms prior to a 1.5 s recovery period. Carbon signals were then observed after a nonselective 90° pulse.

2.4. Observing hyperpolarized signals

Small tip angle, direct detection experiments were collected using a simple pulse of “x” phase with a 5° tip angle (1.0 μs pulse width) immediately followed by acquisition of ^{13}C signals. The spectral width for these ^{13}C observe experiments was 35 kHz. 8192 complex points were collected while decoupling both D and H nuclei with continuous wave and waltz schemes [19], respectively.

Indirect detection of hyperpolarized ^{13}C magnetization was achieved as described before, except using the circuitry for ^{13}C rather than ^{15}N [10]. In these experiments, 10 Units of ALT were used to collect spectra with a spectral width of 6 kHz and 2000 complex points; the time interval between repetitions was varied.

3. Results

3.1. Direct detection of ALT activity

The ALT mechanism was probed initially with hyperpolarized ^{13}C2-pyruvate. Spectra of hyperpolarized ^{13}C2-pyruvate and the ^{13}Cα-alanine product, shown in Fig. 2, were collected every 1.2 s in a direct ^{13}C-detected experiment by sampling a small proportion of the magnetization (<1%). Reaction progress as represented in heights of peaks corresponding to pyruvate and alanine is depicted in Fig. 2b. The pyruvate signal at 206 ppm decays due to a combination of spin relaxation, losses due to sampling, and to a lesser extent enzyme-catalyzed conversion to alanine. The signal from the hydrate form of pyruvate, which is in rapid equilibrium with the keto-form at 94 ppm, parallels this loss. The alanine signal at 51 ppm shows a slight rise before decay due to the enzymatic production of alanine, but decay quickly dominates due to the unfavorable relaxation properties of the alanine Cα nucleus. The C1 signal of pyruvate, resulting from natural ^{13}C abundance, is present at ~171 ppm, the other signals likely originate from unenriched components of the hyperpolarization buffer. It is noteworthy that we do not see natural abundance peaks for the C3 methyl carbon in this experiment or another experiment with 30-fold more pyruvate (data not shown), presumably because the protonated carbon relaxes too quickly to store enhanced polarization. This appears to be the case even though methyl relaxation should be slowed by the effects of rapid methyl rotation [20].

The storage and magnetization lifetime properties of ^{13}C3 should be enhanced by replacing protons (H) with deuterons (D) that have just 1/6th the magnetogyric ratio. Consistent with participation of an enamine isoform in the mechanism presented above, deuteron incorporation into alanine following the incubation of ALT with $^{13}CH_3$-pyruvate and glutamate in D_2O was observed through the appearance of isotope-shifted CDH_2 and CD_2H peaks (data not shown). Carbon resonances are shifted additively by directly-bonded deuterons to a higher frequency when compared to $^{13}C(H_3)$. This isotope effect will be utilized later to further investigate the ALT mechanism. Interestingly, exchange into the pyruvate methyl group during the initial phase of the reaction was not observed, either due to the lack of efficient reversal of mechanistic steps prior to enamine incorporation or rapid relaxation of the fully protonated methyl group (data not shown).

When using $^{13}CD_3$-pyruvate as a starting material, the pyruvate $C3D_3$ signal at 26.2 ppm is easily observed (Fig. 2c) and now decays at about the same rate as the pyruvate C2 signal. Three additional lower intensity peaks to the left of the main methyl peak are also now observed. These correspond to the three additional methyl isotopologues, CD_2H, CDH_2, and CH_3, which based on analysis prior to enzyme action, result from incomplete H/D exchange during our preparation of deuterated pyruvate. A clear accumulation of an alanine Cβ methyl signal was also observed as a consequence of the slow relaxation of deuterated methyls and prolonged polarization storage (dotted line, Fig. 2d). A comparison of the ^{13}Cα(H) signal (red[1] line, Fig. 2b) with the alanine ^{13}Cβ (D_3) signal (dotted line, Fig. 2d), indicates a significant advantage in monitoring a Cβ D3 signal as compared to the protonated Cα of the alanine product. There are further advantages to be gained from an analysis of the isotopologue peaks seen to the left of the main alanine methyl peak.

3.2. Detecting nascent alanine

Isotopologue distributions for the alanine methyl group as presented above clearly show that in the process of producing alanine, protons replaced deuterons on the Cβ methyl group. This can be seen by comparing the data on C3 of pyruvate to that on Cβ of alanine as shown

[1]For interpretation of color in Fig. 2, the reader is referred to the web version of this article.

in Fig. 3a and b. However, due to limitations of looking at alanine which has accumulated from the beginning of the experiment, combined with the effects of spin relaxation, when using this small tip-angle approach, it is difficult to quantitate the production of various isotopologues. To appreciate this limitation, compare the apparent distribution of alanine isotopologues on the first scan (Fig. 3b) to that at a later scan where the fully deuterated form appears to dominate (Fig. 3c). The domination at long times is likely the result of faster relaxation, and thus greater loss of signal, for the alanine Cβ forms with greater proton content. The experimental design samples magnetization from the total pool of alanine, regardless of when it was formed. Thus, the cumulative losses of magnetization from protonated forms will bias the measurements towards CD_3. The first point provides the best possible distribution measurement but suffers from inefficient mixing and additional instrumental delays following transport of the hyperpolarized substrate.

The relative isotopologue distribution can be more accurately measured by changing the experimental strategy to detect only newly formed alanine. With the enhanced sensitivity of hyperpolarized samples it is possible to recover adequate signal even with short production periods (1.5 s). To achieve this, the alanine signal formed before the recovery period is specifically destroyed by low power continuous-wave irradiation at the alanine methyl frequency in a manner which does not disturb the pool of hyperpolarized pyruvate. The recovery period is short relative to the signal decay for each of the four isotopologues, and thus intensities should only be minimally affected by differences in relaxation rates. As expected, the isotopologue distribution of nascent ^{13}Cβ-alanine showed a greater proportion of forms containing protons than observed previously (Fig. 3d), and their observation allows the number of protons incorporated during one pass through the catalytic cycle to be estimated. Measurements were made within 8 s of reaction initiation and with amounts of substrate and enzyme that will approach chemical equilibrium only after ~3 min. These conditions preserve the assumptions of pseudo-first order conditions by keeping polarized product accumulation at a minimum and allowing only negligible amounts of alanine to recycle to form pyruvate. An analysis of peak intensities revealed that on average, ~0.8 deuterons were exchanged to protons by ALT per catalytic cycle (66% D content at Cβ in alanine, 95% at C3 in pyruvate according to the initial synthesis value).

3.3. Indirect detection of ALT activity

To capitalize upon ALT-catalyzed D/H exchange as a means of detecting newly formed alanine with further sensitivity enhancement, we adapted an existing pulse sequence [10] to transfer ^{13}C polarization to a proton for detection as shown in Fig. 4. This sequence has a unique property in that it returns the magnetization vector of hyperpolarized, non-protonated carbon nuclei to the $+z$ axis after each acquisition, thus these carbons serve as storage sites until a directly-bonded ^{1}H is chemically added (for more details, see [10]). Our first efforts tuned the sequence to detect magnetization optimally from the 13CβD2H isotopologue (Fig. 4a) using τ_a delays corresponding to the period required for pure carbon transverse coherence to evolve to carbon transverse coherence anti-phase with respect to the directly bonded proton ($1/4J_{CH}$ = 1.97 ms; Fig. 4b). As a result, nearly 100% of the ^{13}Cβ(D_2H) coherence could be transferred to the (^{13}CβD2)H proton while ^{13}Cβ(DH_2) coherence remained on carbon. The ^{13}Cβ(H_3) coherence would be detected with about 2/3 efficiency in this experiment as well, but ALT produces a very small amount (<5%) under conditions of the experiment and therefore contributions from this form are neglected. Hyperpolarized ^{13}C magnetization was then passed to protons, refocused in a second delay with τ_b = 1.97 ms, and detected indirectly with high sensitivity. The sequence was then repeated multiple times to detect additional amounts of ^{13}Cβ(D_2H) alanine as it was formed from the initial bolus of hyperpolarized pyruvate (Fig. 4c). As insignificant amounts of pyruvate are consumed in the course of the experiment, one would expect similar amounts of alanine to be sampled at

each point. Signal intensity in this experiment is then just a function of the D/H exchange rate, the sampling frequency and the decay of pyruvate polarization. The polarization decay is due to spin relaxation of the deuterated pyruvate; the sampling frequency dependence arises because the coherence from deuterated pyruvate is inefficiently returned after each cycle of the pulse sequence. These factors are described in more detail elsewhere [10]. Sampling infrequently, in contrast to what is shown here, will provide somewhat better sensitivity and the greatest opportunity to observe slow events; however, alanine $^{13}C\beta(D_2H)$ relaxation in addition to pyruvate $^{13}C3$ relaxation will still limit application.

From our carbon detect experiments we noted the alanine isotopologue distribution, following a single ALT catalytic cycle, contained as much as 20% $^{13}C\beta(DH_2)$, and possibly 5% $^{13}C\beta(H_3)$. These additional species can, in principle, be detected selectively by indirect detection as well. The simplest approach is to change the τ_a delay to optimize carbon to proton transfer delays for the respective species: $1/4J_{CH}$ = 1.97 ms for CHD_2, $1/8J_{CH}$ = 0.99 ms for CH_2D and $1/12J_{CH}$ = 0.66 ms for the outer lines of CH_3. Spectra from the first three of these samplings at high resolution, as seen in Fig. 5a, showed the expected pattern of alanine signals. The alanine $^{13}C\beta(D_2H)$ methyl appeared as a doublet with a resolved ~7 Hz Hβ–Hα coupling in the spectra collected with $\tau_a = 1/4J_{CH}$ (Fig. 5a, bottom plot). In spectra collected with $\tau_a = 1/8J_{CH}$ or $1/12J_{CH}$ an unequal mixture of $(^{13}C\beta)DH_2$ and $(^{13}C\beta)D_2H$ were resolved, the latter isotopologue signal being found upfield relative to the former due to isotope shifts (Fig. 5a, middle and top plots). It is possible to design sequences that more cleanly return signals from a single isotopologue by changing the τ_a delays for successive cycles of the sequence and adding or subtracting appropriately scaled signals. For example, choosing successive τ_a values of $1/8J_{CH}$ and $3/8J_{CH}$, and subtracting signals that have been scaled for differences in transverse relaxation and polarization decay will yield a pure CH_2D signal.

The total intensity of the detected signals is of some interest as a means of detecting the raw rate of alanine production by alanine transaminase for in-cell or *in vivo* applications. In these applications resolution is not likely to be adequate and neither multiplet structure nor isotope shifts are likely to be resolved. It is clear that of the three delays depicted in Fig. 5b the $1/8J_{CH}$ delay has yielded the best spectrum. This is likely the result of the simultaneous detection of relatively high proportions of $(^{13}C\beta)DH_2$ and $(^{13}C\beta)D_2$-H signals. A direct comparison of indirect detection through ^1H and direct ^{13}C detection is not straight forward. However, our best option is a comparison of the total directly detected CH_2D and CHD_2 lines in the “nascent” alanine spectrum (Fig. 3d) and the $1/8J_{CH}$ delay selection in the indirect detection experiment which detects 100% and 72% of the CH_2D and CHD_2 intensity, respectively (Fig. 5a, 3.3 s). Comparing signal integrals in equally line-broadened spectra (with a 4.0 Hz Gaussian multiplier) on a Hz scale, normalizing amplitudes based on noise, and correcting for differences in product accumulation times, enzyme concentration and polarization levels, the indirectly-detected spectrum is 7.9-fold more sensitive. This result is respectable compared to the 16-fold theoretical advantage, especially considering that we do not detect all CHD_2 intensity and the ^1H detection efficiency of our probe is not quite that of ^{13}C. However, it may be possible to further improve the pulse sequence and experimental protocol as discussed below.

4. Discussion

In summary, several new techniques using hyperpolarized $^{13}C2$- and $^{13}C3D_3$-pyruvate to probe ALT activity have been explored. Direct observation of ^{13}C sites after polarizing the deuterated C3 methyl group of pyruvate showed a significant advantage over polarizing the C2 carbonyl group. This very likely results from favorable relaxation properties of the deuterated methyl group in comparison to that of the C2 carbonyl at high magnetic field.

ALT was also shown to catalyze D/H exchange at the alanine methyl group, incorporating a significant number of protons into the $^{13}CD_3$ moiety per catalytic cycle. This latter observation opens opportunities to probe catalytic mechanisms as well as explore indirect detection as a way of further improving sensitivity of enzyme activity measurements in in-cell and *in vivo* experiments.

4.1. Interpreting the ALT catalytic mechanism

The improved sensitivity offered by hyperpolarization proved important in studying nascent alanine production on the timescale of ~1.5 s and allowed determination of the amount of D/H exchange per cycle with minimal interference from unequal isotopologue polarization decay and reassociation of product with the enzyme. It is possible that a similar determination could have been made by reducing enzyme concentration and acquiring spectra over long periods of time by signal averaging non-hyperpolarized preparations. However, there are certainly situations where background reactions (buffer catalyzed exchange, for example) and significant product reassociation rates would have skewed isotopologue determinations. Moreover, with *in vivo* and in cell determinations, one does not always have the liberty of adjusting enzyme concentrations. Thus, enhanced sensitivity will certainly prove advantageous in future studies.

The catalysis of H/D exchange at the methyl group is interesting as this is not required by the accepted mechanism drawn in Fig. 1. However, the formation of a Schiff base intermediate opens the possibility of interchange with an enamine form (upper part of Fig. 1), allowing exchange of a methyl deuteron as illustrated. It is noteworthy that the products of D/H exchange include all four isotopologues. This suggests the Schiff base – enamine interconversion is not obligatory, and thus enamine formation does not lead directly and efficiently to alanine production. If enamine formation did lead directly to the alanine product, and a non-concerted mechanism existed in which the abstracted deuteron rapidly equilibrated with solvent protons, just a single proton would be introduced to the methyl group and no CβD3 or CβDH2 would be observed. Thus, it is more likely that D/H exchange occurs as a dispensable side reaction that is in equilibrium prior to base-catalyzed proton abstraction from the coenzyme (denoted by a *circled* "*B*" in Fig. 1). The number of protons introduced to the methyl group is then a measure of the rate of equilibration through pathway *B* compared to the rate of product release. Interestingly, with these assumptions we can estimate the relative rates. Data indicate off-pathway enamine equilibration occurs at a rate that is about 0.8 times that of the passage through pathway *B* to alanine. Thus, the formation of the ALT off-pathway intermediate is significant.

It is also informative that we do not see significant levels of methyl protons introduced into pyruvate, suggesting that under our conditions the dissociation of the Schiff base to release pyruvate does not occur at a significant rate compared to alanine formation. Another enzyme using pyruvate and a Schiff base intermediate, *N*-acetylneuraminic acid aldolase, does use the enamine form of a Schiff base as an obligatory intermediate [21]. In this case we found both a higher rate of exchange in the released product (*N*-acetylneuraminic acid) and a higher rate of reversal to release a protonated pyruvate (data not shown). Hence, the pattern of isotopologue production is quite different. There are a great number of other enzymes that share the Schiff base mechanism, including class 1 fructose 1-6 bisphosphate aldolase [22] and most pyridoxal phosphate-dependent enzymes [16]. Differences in proton incorporation patterns may be quite different for these enzymes and exchange signatures may provide a useful specific diagnostic.

4.2. Imaging considerations for using ^{13}C2- or ^{13}C3D$_3$-pyruvate

^{13}C3D$_3$-pyruvate proved superior to the ^{13}C2 form as a substrate for directly ^{13}C detected ALT activity. At high fields in the absence of enzyme and free radicals from the hyperpolarization medium, the ^{13}C3D$_3$ methyl group relaxes at less than half the rate of the ^{13}C2 carbonyl (0.018 s^{-1} vs. 0.045 s^{-1} at 14 T and 25 °C). In practice the considerable slower relaxation rate of ^{13}C3D$_3$ compared to CαH in the product proves to be of more consequence and allowed detection of the alanine product with much higher sensitivity. Metabolism of hyperpolarized ^{13}C2-pyruvate is of considerable interest for *in vivo* monitoring of other reactions [23,24] and the results reported here indicate ^{13}C3D$_3$-pyruvate may prove superior for some of these applications as well. Indirect detection after D/H exchange into the methyl group could offer additional advantages for *in vivo* application, but there are clearly obstacles to overcome with the complexity of the pulse sequence and the need for deuterium decoupling.

Comparing the relative sensitivities of the current indirect and direct detected experiments revealed the signal to noise in the indirectly detect experiment was 7.9-fold superior to the direct-detect experiment (Figs. 3d and 5a, 3.3 s), but below the 16-fold theoretical enhancement. This may be due to several factors. First, convective currents and residual turbulence from pyruvate injection into the large 8 mm NMR tube can cause significant losses, especially when pulsed field gradients and refocusing pulses are used (Fig. 4b) [25,26]. Second, the probe used here is not optimal for ^{1}H detection (experimentally a factor of 40 superior proton detection, compared to a 64-fold theoretical advantage). Third, Hα–Hβ coupling evolution during the τ delays is not removed by the current version of the pulse sequence and can cause some additional loss. There are things that can be done to avoid some of these effects and optimize future experiments. In particular, it is possible to minimize convective and turbulent currents by introducing baffles in the sample tube. The refocusing elements (τ_b) can also be kept at the shortest odd multiple of 1/4J and the effect of coherence decay due to gradients in this period minimized by switching to a non-gradient water suppression technique. Hence, we believe that sensitivity improvement seen in indirect detection experiments can be improved in the future.

Acknowledgments

Funding sources

This research was funded by grants from the National Center for Research Resources (5P41RR005351-23) and the National Institute of General Medical Sciences (8 P41 GM103390-23) from the National Institutes of Health awarded to J.H.P., and a Kirschstein NRSA Fellowship F32AR058084 awarded to A.W.B. The content is solely the responsibility of the authors and does not necessarily reflect the views of the NIH.

We thank Urvesh Patel for his preparation of the sodium ^{13}C3D$_3$-pyruvate.

Abbreviations

ALT	alanine transaminase
D	deuteron, deuterium atom
H	proton, hydrogen atom

References

1. Ardenkjaer-Larsen JH, Fridlund B, Gram A, Hansson G, Hansson L, Lerche MH, Servin R, Thaning M, Golman K. Increase in signal-to-noise ratio of >10,000 times in liquid-state NMR. Proc Natl Acad Sci USA. 2003; 100:10158–10163. [PubMed: 12930897]

2. Merritt ME, Harrison C, Storey C, Jeffrey FM, Sherry AD, Malloy CR. Hyperpolarized ^{13}C allows a direct measure of flux through a single enzyme-catalyzed step by NMR. Proc Natl Acad Sci USA. 2007; 104:19773–19777. [PubMed: 18056642]
3. Witney TH, Brindle KM. Imaging tumour cell metabolism using hyperpolarized ^{13}C magnetic resonance spectroscopy. Biochem Soc Trans. 2010; 38:1220–1224. [PubMed: 20863288]
4. Kurhanewicz J, Vigneron DB, Brindle K, Chekmenev EY, Comment A, Cunningham CH, DeBerardinis RJ, Green GG, Leach MO, Rajan SS, Rizi RR, Ross BD, Warren WS, Malloy CR. Analysis of cancer metabolism by imaging hyperpolarized nuclei: prospects for translation to clinical research. Neoplasia. 2011; 13:81–97. [PubMed: 21403835]
5. Xu T, Mayer D, Gu M, Yen YF, Josan S, Tropp J, Pfefferbaum A, Hurd R, Spielman D. Quantification of in vivo metabolic kinetics of hyperpolarized pyruvate in rat kidneys using dynamic ^{13}C MRSI. NMR Biomed. 2011; 24:997–1005. [PubMed: 21538639]
6. Aime S, Gobetto R, Reineri F, Canet D. Hyperpolarization transfer from parahydrogen to deuterium via carbon-13. J Chem Phys. 2003; 119:8890–8896.
7. Chekmenev EY, Norton VA, Weitekamp DP, Bhattacharya P. Hyperpolarized (1)H NMR employing low gamma nucleus for spin polarization storage. J Am Chem Soc. 2009; 131:3164–3165. [PubMed: 19256566]
8. Allouche-Arnon H, Gamliel A, Barzilay CM, Nalbandian R, Gomori JM, Karlsson M, Lerche MH, Katz-Brull R. A hyperpolarized choline molecular probe for monitoring acetylcholine synthesis. Contrast Media Mol Imaging. 2010; 6:139–147. [PubMed: 21698772]
9. Allouche-Arnon H, Lerche MH, Karlsson M, Lenkinski RE, Katz-Brull R. Deuteration of a molecular probe for DNP hyperpolarization – a new approach and validation for choline chloride. Contrast Media Mol Imaging. 2011; 6:499–506. [PubMed: 22144028]
10. Barb AW, Hekmatyar SK, Glushka JN, Prestegard JH. Exchange facilitated indirect detection of hyperpolarized 15ND2-amido-glutamine. J Magn Reson. 2011; 212:304–310. [PubMed: 21824795]
11. Qu W, Zha Z, Lieberman BP, Mancuso A, Stetz M, Rizzi R, Ploessl K, Wise D, Thompson C, Kung HF. Facile synthesis [5-(13)C-4-(2)H(2)]-L-glutamine for hyperpolarized MRS imaging of cancer cell metabolism. Acad Radiol. 2011; 18:932–939. [PubMed: 21658976]
12. Kennedy BWC, Kettunen MI, Hu DE, Brindle KM. Probing lactate dehydrogenase activity in tumors by measuring hydrogen/deuterium exchange in hyperpolarized L-[1-C-13, U-H-2]lactate. J Am Chem Soc. 2012; 134:4969–4977. [PubMed: 22316419]
13. Albers MJ, Bok R, Chen AP, Cunningham CH, Zierhut ML, Zhang VY, Kohler SJ, Tropp J, Hurd RE, Yen YF, Nelson SJ, Vigneron DB, Kurhanewicz J. Hyperpolarized ^{13}C lactate, pyruvate, and alanine: noninvasive biomarkers for prostate cancer detection and grading. Cancer Res. 2008; 68:8607–8615. [PubMed: 18922937]
14. Sleisenger, MH.; Feldman, M.; Friedman, LS.; Brandt, LJ. Sleisenger & Fordtran's Gastrointestinal and Liver Disease: Pathophysiology, Diagnosis, Management. 8. Saunders; Philadelphia: 2006.
15. Oshima T, Tamiya N. Mechanism of transaminase action. Biochem J. 1961; 78:116–119. [PubMed: 13731421]
16. Walsh, C. Enzymatic Reaction Mechanisms. W.H. Freeman; San Francisco: 1979.
17. Toney MD. Reaction specificity in pyridoxal phosphate enzymes. Arch Biochem Biophys. 2005; 433:279–287. [PubMed: 15581583]
18. Babu UM, Johnston RB. D2O-alanine exchange reactions catalyzed by alanine racemase and glutamic pyruvic transminase. Biochem Biophys Res Commun. 1974; 58:460–466. [PubMed: 4209898]
19. Shaka AJ, Keeler J, Frenkiel T, Freeman R. An improved sequence for broadband decoupling – Waltz-16. J Magn Reson. 1983; 52:335–338.
20. Woessner DE. Spin relaxation processes in a 2-Proton system undergoing anisotropic reorientation. J Chem Phys. 1962; 36:1–4.
21. Schauer R, Sommer U, Kruger D, van Unen H, Traving C. The terminal enzymes of sialic acid metabolism: acylneuraminate pyruvate-lyases. Biosci Rep. 1999; 19:373–383. [PubMed: 10763805]

22. Lehninger, AL.; Nelson, DL.; Cox, MM. Lehninger Principles of Biochemistry. 5. W.H. Freeman; New York: 2008.

23. Marjanska M, Iltis I, Shestov AA, Deelchand DK, Nelson C, Ugurbil K, Henry PG. In vivo ^{13}C spectroscopy in the rat brain using hyperpolarized [1-(13)C]pyruvate and [2-(13)C]pyruvate. J Magn Reson. 2010; 206:210–218. [PubMed: 20685141]

24. Hu S, Yoshihara HA, Bok R, Zhou J, Zhu M, Kurhanewicz J, Vigneron DB. Use of hyperpolarized [1-(13)C]pyruvate and [2-(13)C]pyruvate to probe the effects of the anticancer agent dichloroacetate on mitochondrial metabolism in vivo in the normal rat. Magn Reson Imaging. 2012

25. Allerhand A, Addleman RE, Osman D. Ultrahigh resolution NMR. 1. General-considerations and preliminary-results for C-13 NMR. J Am Chem Soc. 1985; 107:5809–5810.

26. Loening NM, Keeler J. Measurement of convection and temperature profiles in liquid samples. J Magn Reson. 1999; 139:334–341. [PubMed: 10423370]

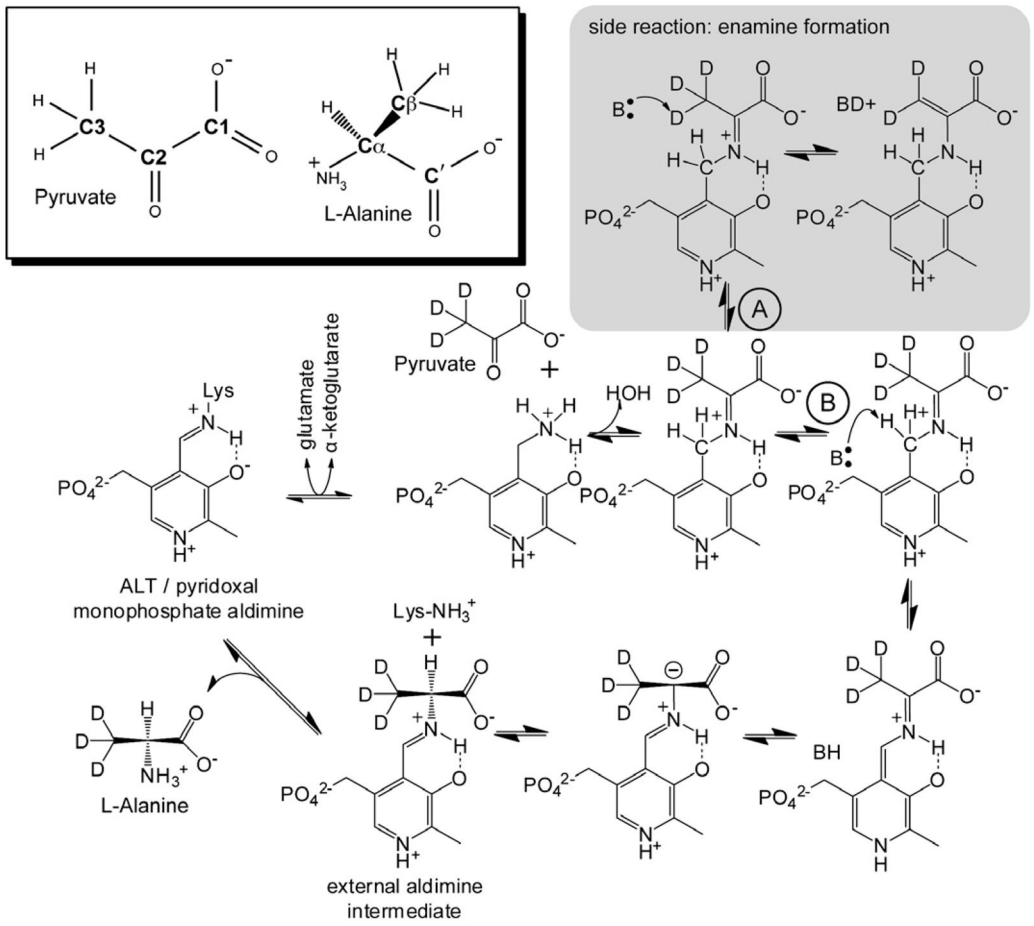

Fig. 1.

Alanine transaminase (ALT) catalytic mechanism. A proposed excursion starting at the *circled* "A" would explain the observed D/H exchange [15–17] and is highlighted with a *grey* background. The inset shows the carbon nomenclature used herein.

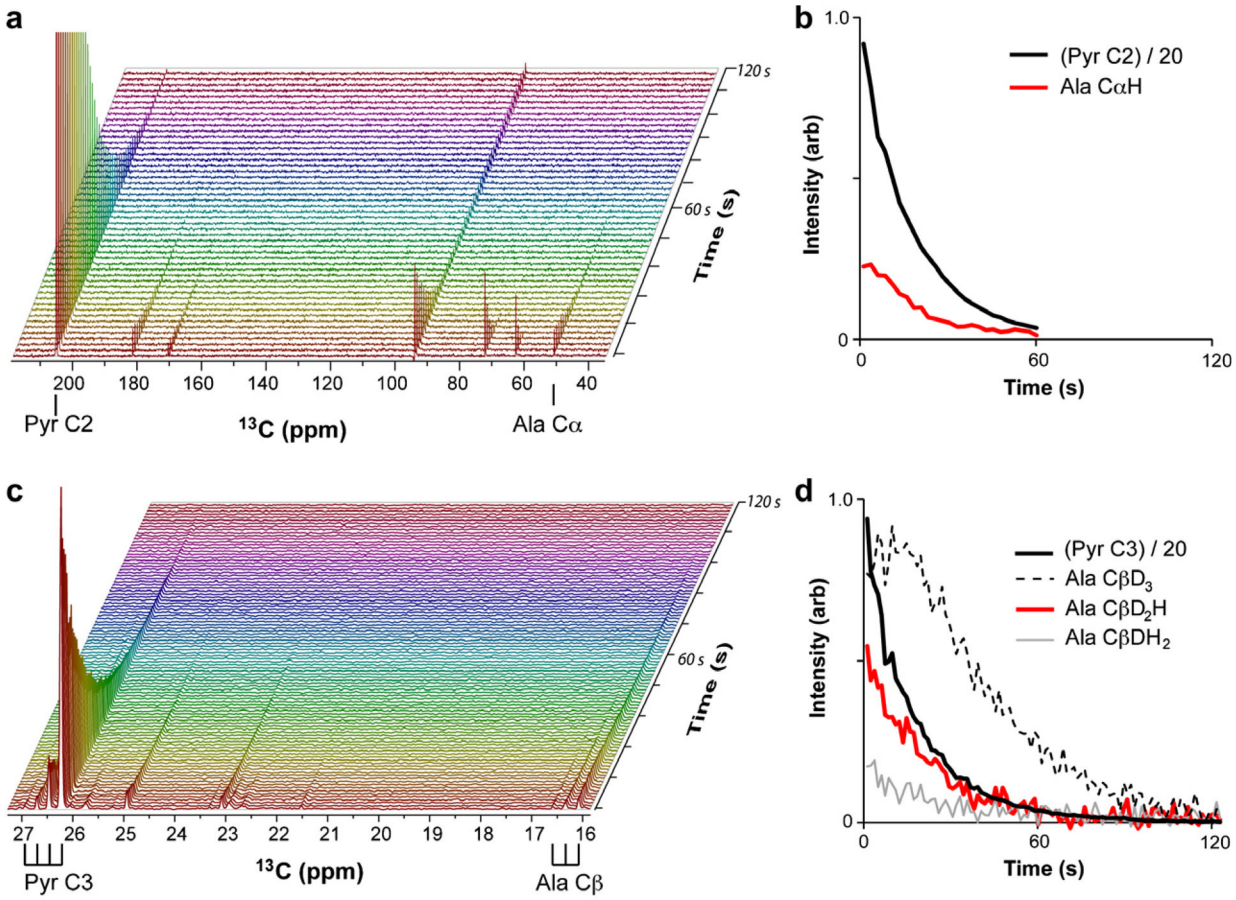

Fig. 2.

Direct ^{13}C observation of ALT activity using hyperpolarized sodium pyruvate. (a) A stacked plot of individual spectra following conversion of hyperpolarized $^{13}C2$-pyruvate into $^{13}C\alpha$-L-alanine. The resonances corresponding to these nuclei are indicated below the horizontal axis. (b) A plot showing observed intensities extracted from the spectra shown in panel (a). (c) A stacked plot of ALT-catalyzed conversion of hyperpolarized $^{13}C3D_3$-pyruvate into $^{13}C\beta$-L-alanine. The resonances corresponding to these nuclei are indicated below the horizontal axis; note the resolution of peaks corresponding to the $^{13}CD_3$ (tallest peak), $^{13}CD_2H$, $^{13}CDH_2$ and $^{13}CH_3$ isotopologues, from right to left, respectively, for both nuclei. (d) A plot showing observed intensities extracted from the spectra shown in panel (c).

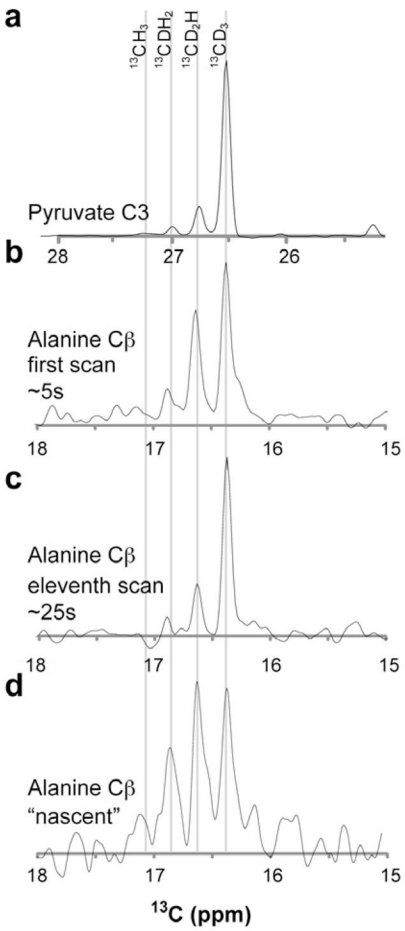

Fig. 3.

Pyruvate isotopologue distributions. (a) The distribution in starting material is consistent with an incomplete deuteration reaction (~95% D). (b) The distribution observed for alanine in the first scan of an ALT reaction is different. (c) This apparent distribution changes throughout the course of an experiment, but is no longer reflective of actual chemical species because magnetization of the heavily protonated forms decays more rapidly. (d) A special experiment designed to reduce the effects of magnetization decay and observe signals from the alanine product that was produced in only 1.5 s is shown.

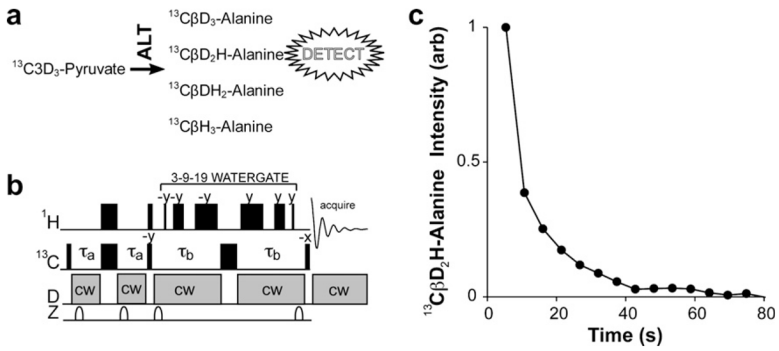

Fig. 4.

ALT-catalyzed D/H exchange permits the indirect detection of hyperpolarized ^{13}C. (a) Four alanine isotologues are produced in ^1H_2O starting from fully deuterated pyruvate. (b) This NMR pulse sequence is designed to transfer hyperpolarized ^{13}C magnetization to nascent ^{1}H for detection and can be tuned to detect these different isotopologues. Details of this pulse sequence can be found in [10]. In panel (c), the delays denoted by τ_a in panel (b) are tuned to detect pure 13CβD2H-L-alanine ($1/4J_{CH}$ = 1.96 ms).

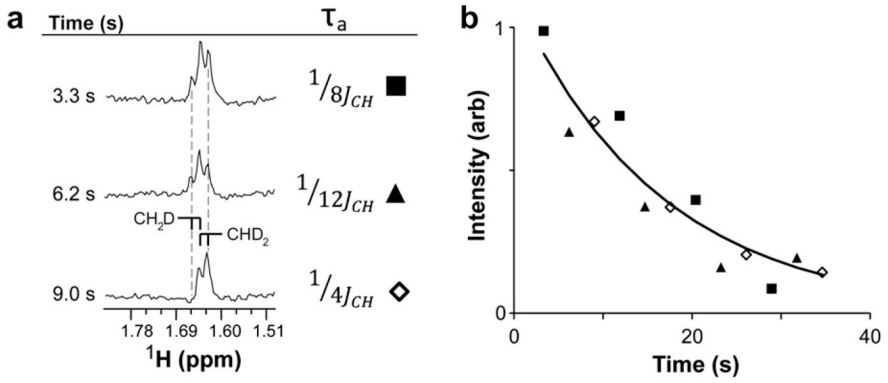

Fig. 5.

Modulating the pulse experiment on-the-fly provides insight into the product isotopologue distribution and identifies a parameter value for optimal sensitivity. (a) A single aliquot of hyperpolarized $^{13}C3D_3$-pyruvate was detected using the experiment in Fig. 3, except values for the delay τ_a were modulated. In the first scan the delay was 0.98 ms to detect a mixture of $^{13}CD_2H$- and $^{13}CDH_2$-alanine; likewise in the second scan with 0.66 ms. The third scan with a 1.96 ms delay will detect magnetization from only the $^{13}CD_2H$ form, recycling the remainder. This three step acquisition pattern was repeated multiple times until the detected hyperpolarized magnetization decayed to undetectable levels. (b) Integral values of product peaks observed using the experimental parameters described in (a). The line represents a best-fit exponential decay of all plotted points.